Supporting Information

Pulse-mediated Electronic Tuning of the MoS_2-perovskite Ferroelectric Field Effect Transistors

Kai-Wen Chen,[†] *Shu-Jui Chang,*[‡] *Ethan. Ying-Tsan Tang,*[⊥] *Chih-Pin Lin,*[#] *Tuo-Hung Hou,*[#] *Chia-Hao Chen,*[§] *and Yuan-Chieh Tseng*[*,†]

[†] Department of Materials Science & Engineering, National Chiao Tung University, 30010, Taiwan

[‡] Intelligent Semiconductor Nano-system Technology Research Center, National Chiao Tung University, Hsinchu 30010, Taiwan

[⊥] Taiwan Semiconductor Research Institute, MarLabs, Hsinchu 30010, Taiwan

[#] Department of Electronics Engineering, National Chiao Tung University, 30010, Taiwan

[§] National Synchrotron Radiation Research Center, Hsinchu 30076, Taiwan

E-mail address for corresponding author: yctseng21@mail.nctu.edu.tw

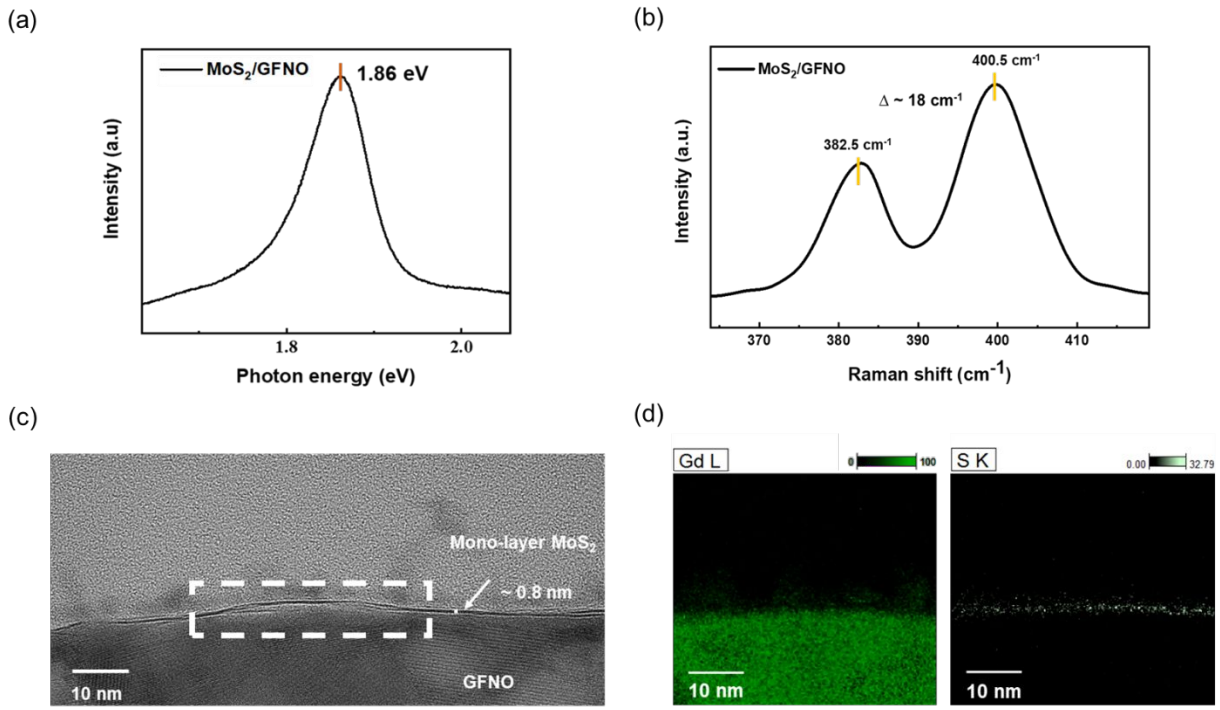

Figure S1: (a) PL spectrum of MoS_2/GFNO showing peak maximum at 1.86 eV; this corresponds to a mono-layer MoS_2. (b) Raman spectrum of MoS_2/GFNO; E^1_{2g} and A_{1g} peak separation (~18 cm^{-1}) indicates MoS_2 is mono-layer. (c) cross-sectional TEM; (d) EDS mapping of Gd and S.

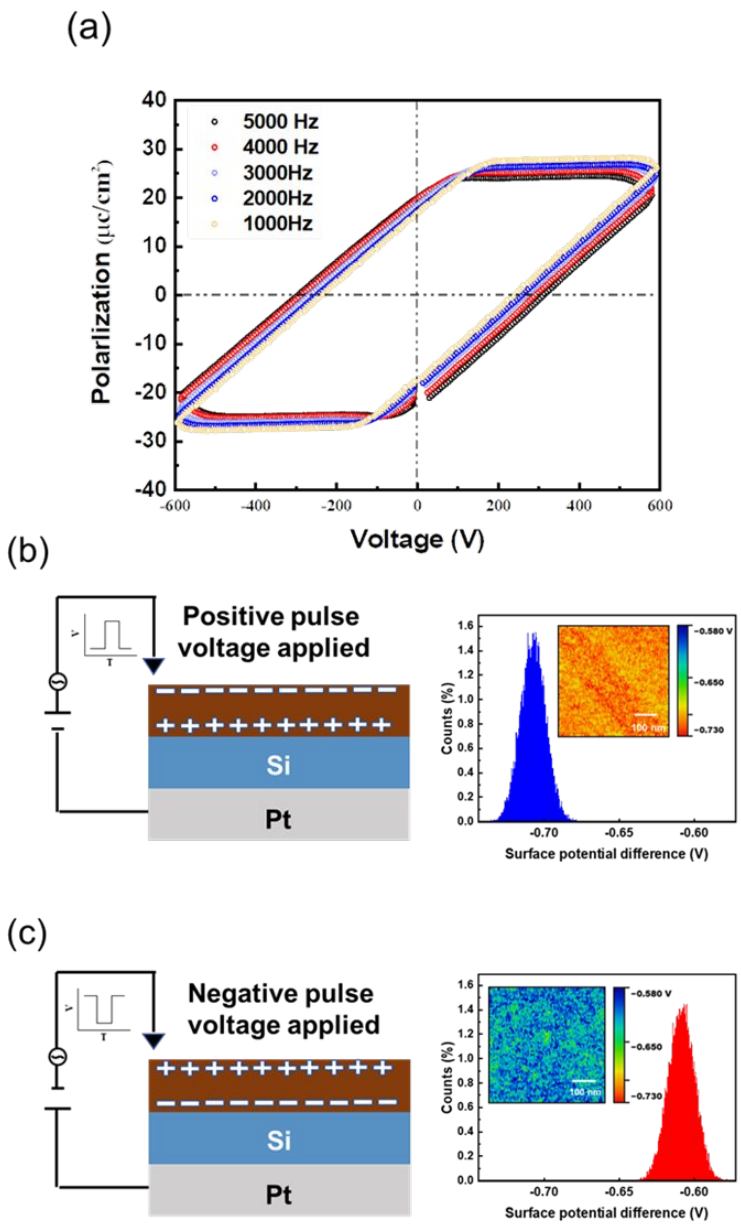

Figure S2(a): Frequency-dependent polarization switching (from 1000 to 5000 Hz) as a function of electrical field in GFNO (without MoS_2 capping); (b) and (c) are schematic illustrations showing the directions of pulses (+/- 4 volts) used to induce opposing ferroelectric dipole alignment within the GFNO layer (brown color). CPD of two GFNO

states along with corresponding KPFM images (insets) are presented on right side. KPFM maps indicate changes in surface potential during the switch from a positive to a negative pulse, which corresponds to surface band bending induced by the bound charge.

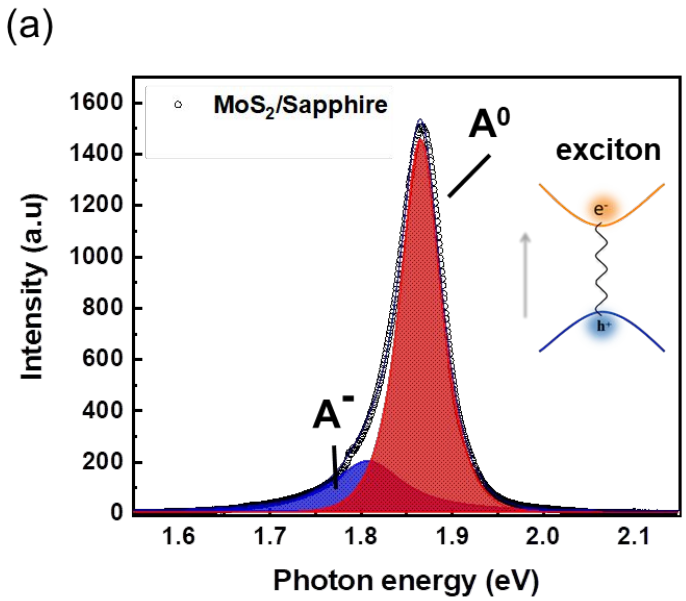

Figure S3: A^0 (neutral) and A^- (trion) integration intensities probed by PL in MoS_2 on (a) sapphire substrate and (b) GFNO substrate. Peak B associated with direct optical transitions from the lowest conduction bands to the highest spin-split valence bands. The neutral exciton (A^0) is the ground state of a charge neutral system, and trions (A^-) are formed by the binding of a free electron to a neutral exciton, represented as $e + A^0 \rightarrow A^-$. We fit the data using three Lorentz functions, respectively corresponding to A^0, A^- and B (peak B associated with direct optical transitions from the lowest conduction bands to the highest spin-split valence bands) peaks. The I_{A^-}/I_{A^0} ratio of MoS_2/GFNO was much higher than that of MoS_2/sapphire, indicating the formation of a large number of trions when MoS_2 was transferred from sapphire to GFNO.

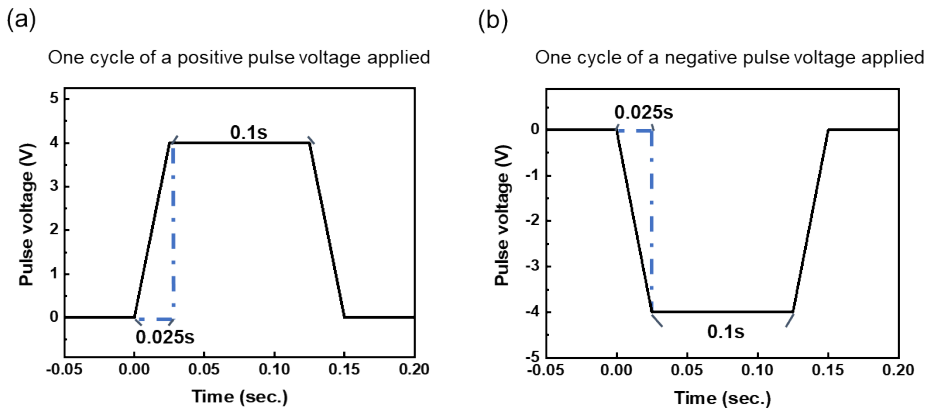

Figure S4: Details of pulse measurements (generated by a Keithley 2400 meter) for (a) positive and (b) negative pulse. Pulse voltage was set at 4 volts. Pulse width and pulse delay time were fixed at 0.1 sec. and 0.025 sec., respectively.

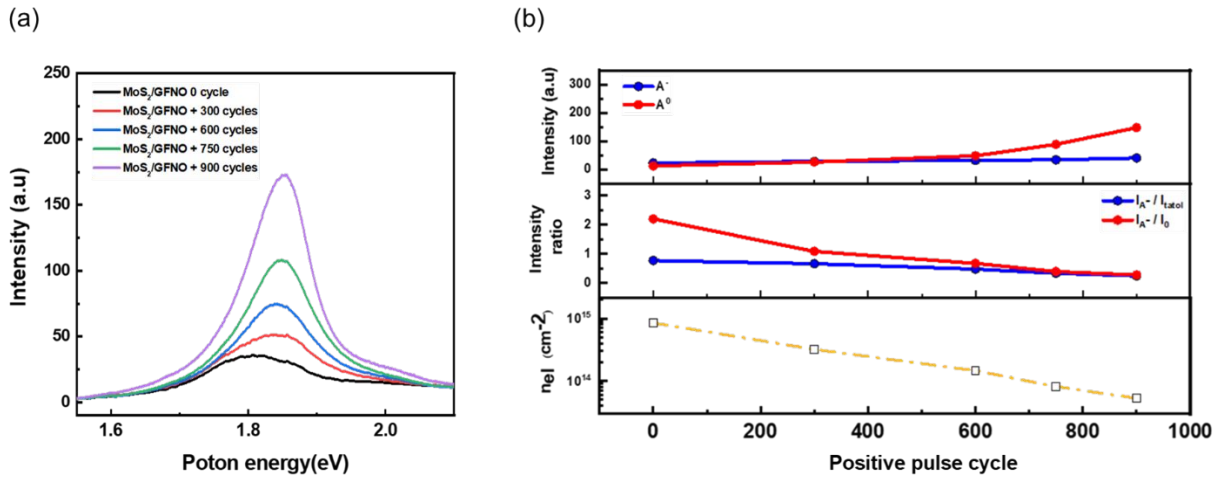

Figure S5: (a) Effects of positive pulse cycle on PL spectra of MoS_2/GFNO device. (b) Top panel: integrated intensity of neutral exciton emissions (A^0) and trion emissions (A^-). Middle panel: intensity ratios of trion emissions (A^-)/neutral exciton emissions (A^0), and

trion emissions (A^-)/[trion emission (A^-) + neutral excitons emissions (A^0)]. Bottom panel: electron density estimated from the three-level model and mass action model.

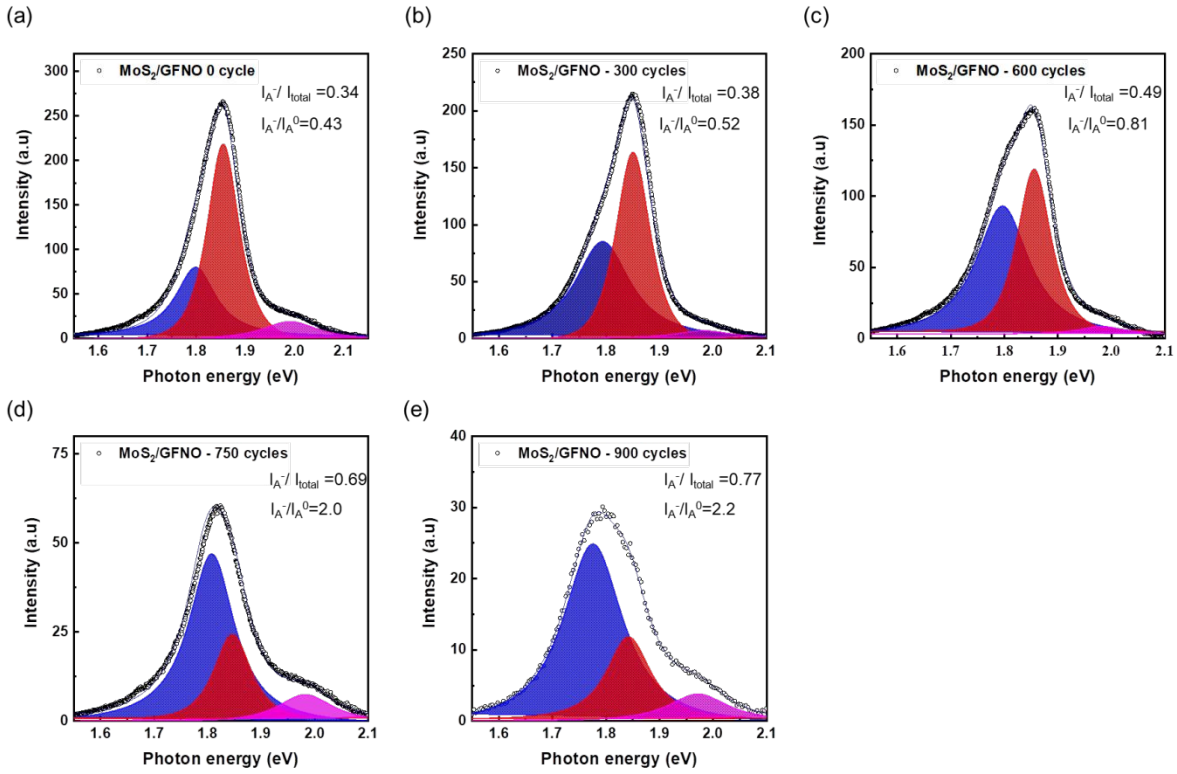

Figure S6: Fitting results of PL spectra from MoS_2/GFNO device responding to the application of various numbers of negative pulse cycles at -4 volts.

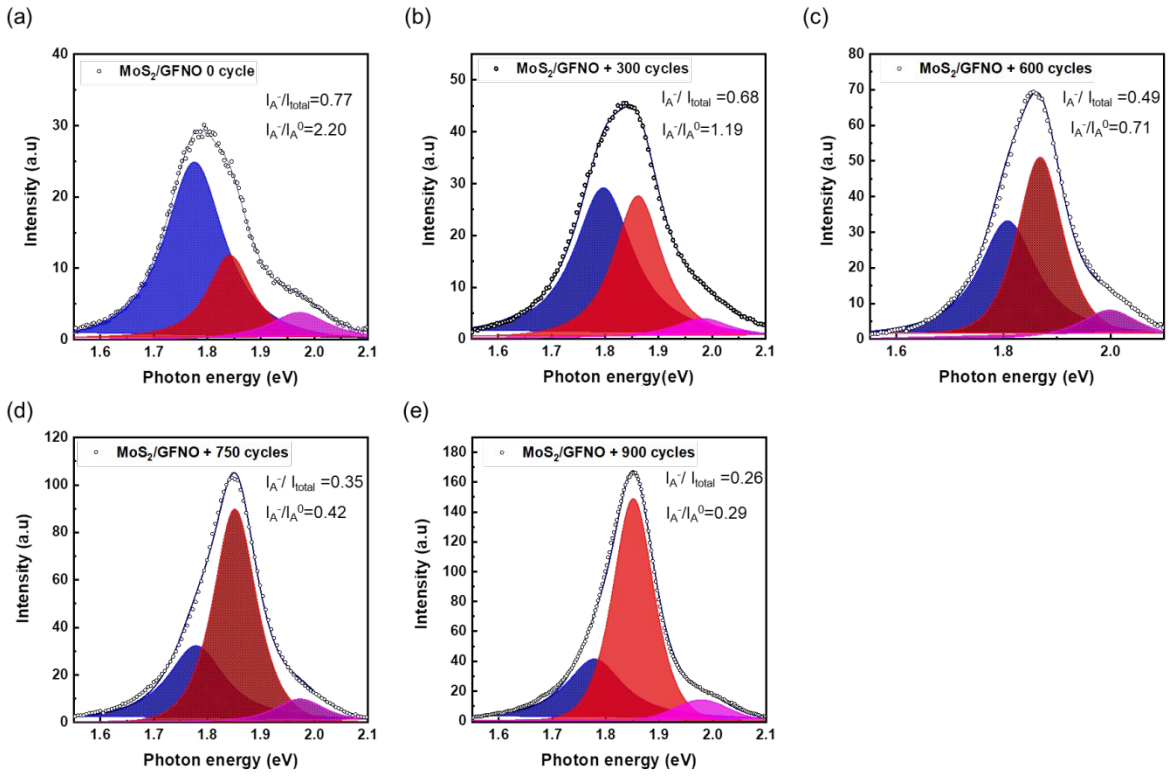

Figure S7: Fitting results of PL spectra from MoS_2/GFNO device responding to the application of various numbers of negative pulse cycles at +4 volts.

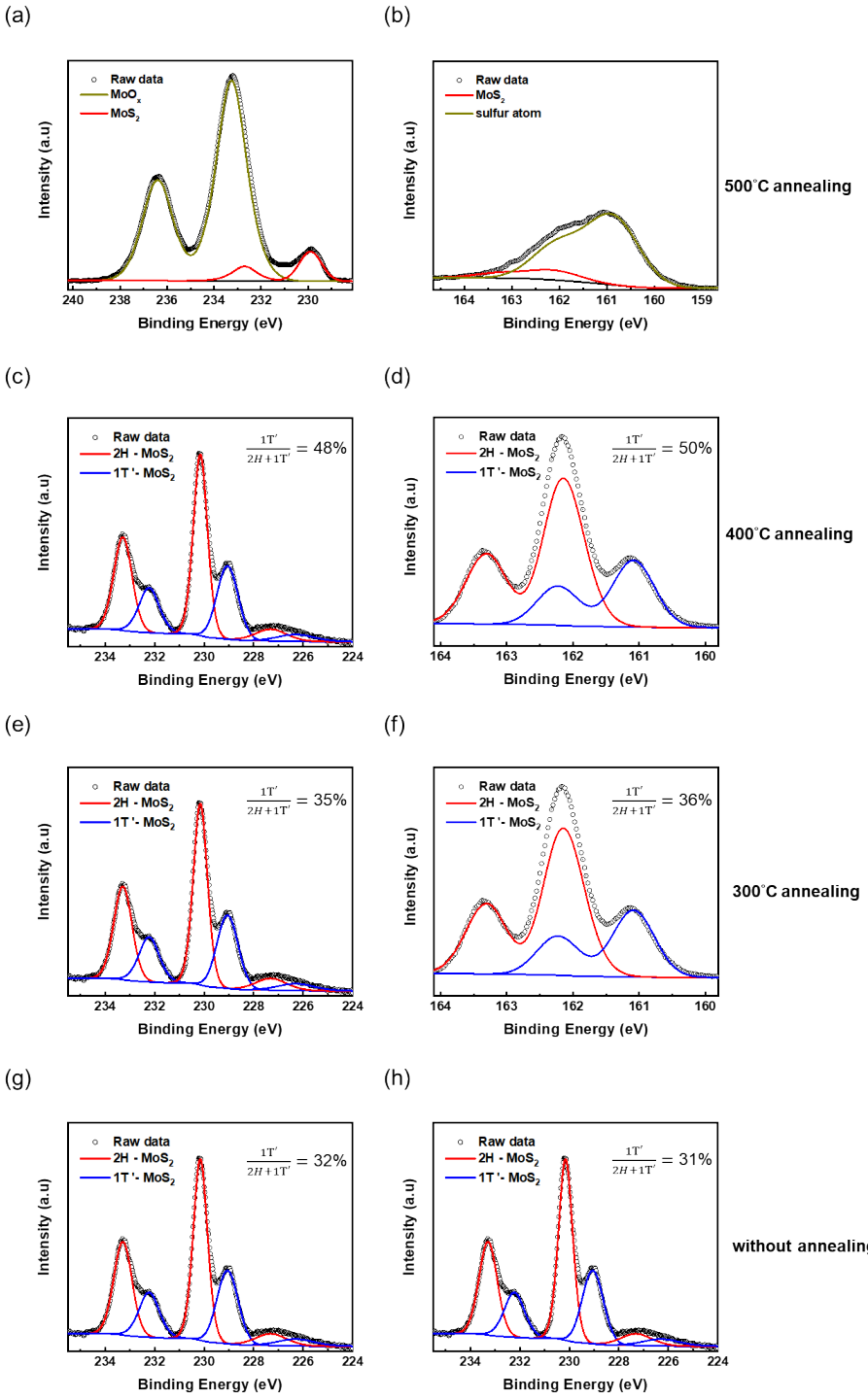

Figure S8: XPS fitting of Mo 3d (a, c, e, g) /S (b, d, f, h). XPS spectra from devices without annealing (g-h) and those that underwent annealing at temperatures of 500 ºC

(a-b), 400 ºC (c-d), 300 ºC (e-f), with each condition induced by 900 pulse cycles at -4 volts

ΔF_γ	0.86 eV/f.u [1]
ΔS_γ	0.1 meV/f.u.[2]
Ps	0.28μC/cm[3]

Table S1: The parameters of Helmholtz free energy calculation in Fig.4. References (Ref.1~3) relevant to the calculations of ΔF_γ (Helmholtz free energy), ΔS_γ (surface energy) and *Ps* (saturated ferroelectric polarization) are given at the end of the supporting information.

	Positive pulse	**Negative pulse**

Core level Peak	2H- intrinsic	2H- extrinsic	2H-MoS_2	1T'-MoS2
Mo 3*d*	231.11 eV	230.86 eV	231.12 eV	230.36 eV
S 2*p*	163.04 eV	162.78 eV	163.04 eV	162.24 eV

Table S2. Information related to differences in binding energy in Figs. 7 (b) and (c)

Calculation of electron density

It has been reported that for a monolayer of MoS_2, the PL results are modulated by electron doping effects[4]. The relative intensity ratio of trion and neutral exciton emissions from a monolayer of MoS_2 is determined by the type of substrate, which can be attributed to differences in substrate induced electron doping effects. For our calculations, the electron density in MoS_2/GFNO from the analysis of PL intensity of excitons and trions emissions. From the mass action model based on the dynamic equilibrium between

neutral excitons (A^0), free electrons and trions (A^-), we obtained the following relationship:[5-7]

$$\frac{N_{A^0} n_{el}}{N_{A^-}} = (\frac{4m_{A^0}m_e}{\pi h^2 m_{A^-}}) k_\beta T e^{(-\frac{E_b}{k_\beta T})}$$

where k_β is the Boltzmann constant, E_b is the trion binding energy (~20 meV)[8], T is the temperature, and m_e(0.35m_0), m_{A^0}(0.8m_0) and m_{A^0}(1.15m_0) respectively indicate the effective mass of neutral excitons, trions and electrons, where m_0 refers to the mass of free electrons.[9] N_{A^0} and N_{A^-} respectively indicate the populations of neutral excitons and trions, and $n_{el}$is the electron density. To establish the relationship between PL intensity and the population of neutral excitons and trions, we considered a three-level model that includes a trion, an exciton, and the ground state. Based on this model, the PL intensity weight can be related to the population of neutral excitons and trions as follows:

$$\frac{I_{A^-}}{I_{total}} = \frac{I_{A^-}}{I_{A^-} + I_{A^0}} = \frac{\frac{\gamma_{A^-} N_{A^-}}{\gamma_{A^0}\ N_{A^0}}}{1 + \frac{\gamma_{A^-} N_{A^-}}{\gamma_{A^0}\ N_{A^0}}}$$

where $I_{A^0}$and I_{A^-} respectively indicate the integrated PL intensity of neutral excitons and trions, and $\gamma_{A^0}$and γ_{A^-} respectively indicate the relative decay rates of neutral excitons and trions. The value of $\frac{\gamma_{A^-}}{\gamma_{A^0}}$ is ~ 0.15 based on the findings of Mouri et al.[10] The three level model can be combined with the mass action model as follows:

$$n_{el} = \frac{\frac{I_{A^-}}{I_{total}}}{\frac{\gamma_{A^-}}{\gamma_{A^0}}(1 - \frac{I_{A^-}}{I_{total}})}\left[(\frac{4m_{A^0}m_e}{\pi h^2 m_{A^-}})k_\beta T e^{(-\frac{E_b}{k_\beta T})}\right] \text{(Eq. S1)}$$

(1) Reshak, A. H.; and Auluck, S. Calculated optical properties of 2H-MoS_2 intercalated with lithium. *Phys. Rev. B* **2003**, 68, 125101.

(2) Kretschmer S.; Komsa, H. P.; Bøggild, P.; Krasheninnikov, A. V. Structural Transformations in Two-Dimensional Transition-Metal Dichalcogenide MoS_2 under

an Electron Beam: Insights from FirstPrinciples Calculations. *J. Phys. Chem. Lett.* **2017**, 8, 3061-3067.

(3) Shirodkar, S. N.; Waghmare, U. V. Emergence of Ferroelectricity at a Metal-Semiconductor Transition in a 1T Monolayer of MoS_2. *Phys. Rev. Lett.* **2014**, 112, 157601.

(4) Li, Y.; Qi, Z.; Liu, M.; Wang, Y.; Cheng, X.; Zhang, G.; Sheng, L. Photoluminescence of Monolayer MoS_2 on $LaAlO_3$ and $SrTiO_3$ Substrates. *Nanoscale* **2014**, 6, 15248–15254.

(5) Siviniant, J.; Scalbert, D.; Kavokin, A. V.; Coquillat, D.; Lascaray, J.-P. Chemical Equilibrium between Excitons, Electrons, and Negatively Charged Excitons in Semiconductor Quantum Wells. *Phys. Rev. B* **1999**, *59*, 1602–1604.

(6) Ross, J. S.; Wu, S.; Yu, H.; Ghimire, N. J.; Jones, A. M.; Aivazian, G.; Yan, J.; Mandrus, D. G.; Xiao, D.; Yao, W.; et al. Electrical Control of Neutral and Charged Excitons in a Monolayer Semiconductor. *Nat Commun.* **2013**, *4*, 1474.

(7) Ron, A.; Yoon, H. W.; Sturge, M. D.; Manassen, A.; Cohen, E.; Pfeiffer, L. N. Thermodynamics of free trions in mixed type GaAs/AiAs quantum wells F, *Solid State Commun.* **1996**, *97*, 741-745.

(8) Mak, K. F.; He, K.; Lee, C.; Lee, G. H.; Hone, J.; Heinz, T. F.; Shan, J. Tightly Bound Trions in Monolayer MoS_2. *Nature Mater* **2013**, *12*, 207–211.

(9) Cheiwchanchamnangij, T.; Lambrecht, W. R. L. Quasiparticle Band Structure Calculation of Monolayer, Bilayer, and Bulk MoS_2. *Phys. Rev. B* **2012**, *85*, 205302.

(10) Mouri, S.; Miyauchi, Y.; Matsuda, K. Tunable Photoluminescence of Monolayer MoS_2 via Chemical Doping. *Nano Lett.* **2013**, *13*, 5944–5948.